

Magnetic and structural phase transition at 363.7 K in tetramethylammonium hexacyanotrimethylenecyclopropanide

S. C. Abrahams, H. E. Bair, F. J. DiSalvo, and P. Marsh
AT&T Bell Laboratories, Murray Hill, New Jersey 07974

L. A. Deuring

Chemistry Department, Columbia University, New York, New York 10027

(Received 4 October 1983)

Deeply colored triclinic crystals of tetramethylammonium hexacyanotrimethylenecyclopropanide $[(\text{Me}_4)\text{N}^+(\text{HCTMCP})^-]$ are diamagnetic at low temperature even though salts of the singly charged anion are expected to be paramagnetic. The magnetic susceptibility increases above 200 K with a pronounced inflection near 360 K: The crystal becomes weakly paramagnetic at higher temperatures. The heat capacity shows this phase transition is at 363.7 K with corresponding entropy increase of about $3.4 \text{ J mol}^{-1} \text{ K}^{-1}$. Two triclinic crystal axes that differ in length by 0.53 \AA at room temperature become identical at $\sim 365 \text{ K}$; two lattice angles that differ by 3.15° at room temperature also become identical at the phase transition. The corresponding thermal-expansion coefficients are fitted by third-order polynomials; all expansion coefficients are linear above $\sim 365 \text{ K}$. The volume increases linearly from 294 to 407 K, but with unit-cell doubling at the phase transition. Large exchange interactions between $(\text{HCTMCP})^-$ anions are necessary to explain the magnetic data and may be a driving force for the structural phase transition at 363.7 K.

INTRODUCTION

Preparation and characterization of purely organic ferromagnetic crystals is of considerable interest. In addition to opening a major new group of magnetic materials, the study of such materials would provide valuable insight into the nature of magnetic interactions between molecular systems. Several possible organic ferromagnetic materials have been proposed,¹⁻⁴ including infinitely large alternant molecules,² radical-polyradical pair systems,³ and ionic complexes of planar cyclic conjugated systems of threefold or higher symmetry.⁴ An anionic component of the latter type of proposed ferromagnetic is the radical anion of hexacyanotrimethylenecyclopropane $[(\text{HCTMCP})^-]$, first synthesized by Fukunaga.⁵ Such ferromagnetic charge-transfer materials would have an unpaired spin on both cation and anion, but one of the ions when further reduced or oxidized must be in the triplet state.⁴ The redox potentials of both ions must be similar for significant mixing of the different charge-transfer states. The redox potential of $(\text{HCTMCP})^-$ is close to that of several cations with a triplet "excited" charge-transfer state. In examining the properties of $(\text{HCTMCP})^-$, the expected normal Curie-Weiss behavior for the magnetic susceptibility of $(\text{Me}_4)\text{N}^+(\text{HCTMCP})^-$ was instead found to be rather complicated as indicated below.

PREPARATION AND CRYSTAL GROWTH

Preparation of $(\text{Me}_4)\text{N}^+(\text{HCTMCP})^-$ was a four-stage process. First the bis(tetrabutylammonium) $[(\text{Bu}_4)\text{N}_2^{2+}]$ salt of $(\text{HCTMCP})^-$, $\text{C}_{44}\text{H}_{72}\text{N}_8$, was synthesized by Fukunaga's method.⁵ Repeated recrystallization from

ethyl acetate:acetonitrile (3:1) gave colorless prisms with a melting point 478–478.5 K. The disodium salt of $(\text{HCTMCP})^-$ was formed by reaction of $(\text{Bu}_4)\text{N}_2^{2+}$ with a large excess of NaI in acetonitrile. The resulting air-sensitive white solid was converted to the $(\text{Me}_4)\text{N}_2^{2+}$ salt by reaction with a large excess of $(\text{Me}_4)\text{NBr}$ in aqueous solution. Finally, the $(\text{Me}_4)\text{N}_2^{2+}$ salt was dissolved in absolute ethyl alcohol (EtOH) (5.25 g in 100 ml) and Br_2 (0.5 ml in 20 ml absolute EtOH) was added with stirring, to give a blue precipitate.

The blue solid was rinsed with water, dried, and dissolved in acetonitrile. Following filtration, crystallization by vapor diffusion of chloroform into the solution at room temperature produced crystals of maximum dimensions $2.6 \times 0.8 \times 0.2 \text{ mm}$. Rinsing with chloroform and air-drying resulted in very deep reddish-purple⁶ prismatic crystals, of high mechanical fragility. Crystal density, by flotation in CCl_4 +hexane, was determined to be 1.19 g cm^{-3} . $(\text{Me}_4)\text{N}^+(\text{HCTMCP})^-$ is stable on prolonged exposure to air and sunlight, although possibly significant changes in the uv and ir spectra were noted after extended (19 d) heating to 386 K. Chemical analysis for $(\text{Me}_4)\text{N}^+(\text{HCTMCP})^-$ found C, 63.60% and 63.86%; H, 4.23% and 4.01%; N, 32.39% and 32.52%, compared with the calculated C, 63.57%; H, 4.00%; N, 32.43% for $\text{C}_{16}\text{H}_{12}\text{N}_7$.

MAGNETIC SUSCEPTIBILITY TEMPERATURE DEPENDENCE

Experimental values for the magnetic susceptibility of $(\text{Me}_4)\text{N}^+(\text{HCTMCP})^-$, uncorrected for the diamagnetic contribution, are given as a function of temperature in Fig. 1. Temperature-independent diamagnetism clearly

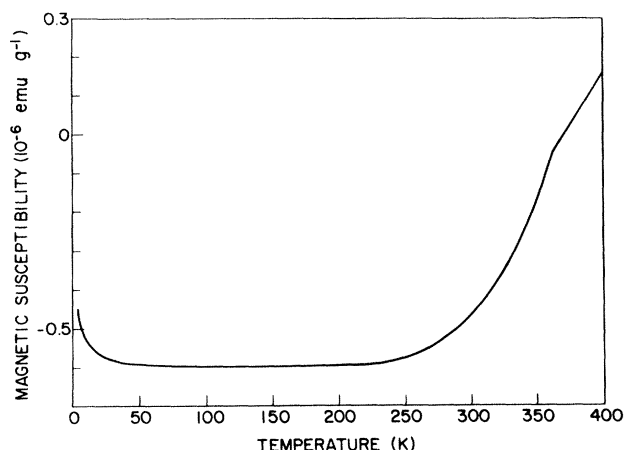


FIG. 1. Magnetic susceptibility of $(\text{Me}_4)\text{N}^+(\text{HCTMCP})^-$ between 4.2 and 400 K.

predominates until about 220 K, apart from a very-low-temperature Curie-impurity component: This "impurity" is consistent with a paramagnetic species ($S = \frac{1}{2}, g = 2$) at a concentration of 10^{-4} . Above 220 K, the susceptibility χ_M rises rapidly by a total of $0.24 \times 10^{-3} \text{ emu mol}^{-1}$ at 400 K, the highest temperature sampled. Examination of Fig. 1 reveals a magnetic transition at about 362 K. The susceptibility of $(\text{Me}_4)\text{N}^+(\text{HCTMCP})^-$ would follow a Curie law with $\chi = C/T + \chi_0$ (χ_0 is the core diamagnetism) if the magnetic moments on the anions were completely uncoupled. The Curie part would lead to a paramagnetic contribution at 400 K of about $10^{-3} \text{ emu mol}^{-1}$, assuming $S = \frac{1}{2}, g = 2$. The actual paramagnetic increase at 400 K is only 25% of this value and it decreases with decreasing temperature instead of increasing as the Curie law predicts. By contrast, the data clearly indicate the spins to be strongly antiferromagnetically coupled, and the increasing paramagnetism at 400 K indicates the exchange temperature is on the order of 500 K.

All anion molecular planes in the triclinic $(\text{Me}_4)\text{N}^+(\text{HCTMCP})^-$ structure are parallel and pack to form sheets slightly inclined to the plane normal direc-

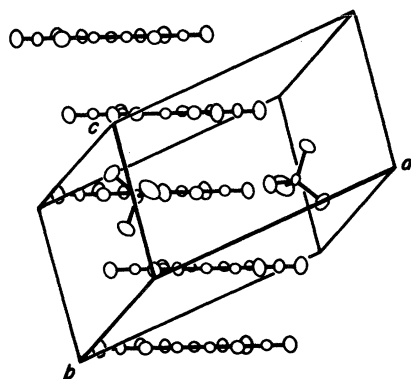


FIG. 2. Packing arrangement of parallel planar $(\text{HCTMCP})^-$ anions in $(\text{Me}_4)\text{N}^+(\text{HCTMCP})^-$ at 294 K with outline of one unit cell. $(\text{Me}_4)\text{N}^+$ cations are shown only within this cell. Each anion shown forms part of a stranded sheet (see Ref. 7).

tion.⁷ There are two types of short (about 3.25 Å) interanionic contact: Those nearly parallel to the molecular plane are $\text{N} \cdots \text{N}$ contacts, those nearly normal to this direction are $\text{C} \cdots \text{C}$ and $\text{C} \cdots \text{N}$ contacts. Typical non-bonded contact distances between carbon and nitrogen atoms are 3.4–3.6 Å. These short distances⁷ suggest that strong exchange forces exist within the sheets, with weaker exchange in the other dimension, (see Fig. 2). The exchange anisotropy within the sheets, however, cannot be readily inferred. In the one-dimensional limit the susceptibility, which would be of the Bonner-Fisher type,⁸ would have a weak maximum at $T \approx J/k$, where J is the exchange energy and k is Boltzmann's constant. The transition at 364 K could be due to the onset of three-dimensional antiferromagnetic order or possibly to a spin-Peierls transition^{9,10} since there is a strong coupling to a lattice distortion. Although the transition mechanism is not yet certain, it is clear that very large exchange interactions exist between $(\text{HCTMCP})^-$ anions.

ELECTRICAL CONDUCTIVITY

Two- and four-point resistance measurements were made from 295 to 370 K on an acicular crystal of $(\text{Me}_4)\text{N}^+(\text{HCTMCP})^-$ along the elongate direction, approximately normal to the molecular plane of the anion. The resistivity decreases by a factor of about 4 upon increasing the temperature to 370 K but remains greater than $10^4 \Omega \text{ cm}$. The large resistivity values indicate the spins are localized on each molecule.

SPECIFIC HEAT

The heat-capacity, C_p , measurements were made on a 19.71-mg sample of $(\text{Me}_4)\text{N}^+(\text{HCTMCP})^-$ in a Perkin-Elmer differential scanning calorimeter (model DSC-2C) over the temperature range 233–393 K. The sample was encapsulated in an aluminum pan and maintained under a nitrogen flow of $20 \text{ cm}^3 \text{ min}^{-1}$. The melting of two standards, *p*-xylene (286.4 K) and indium (429.78 K), was used to calibrate the DSC temperature scale. Energy calibration was based on the fusion (ΔH_f) of indium [$3.27(1) \text{ kJ mol}^{-1}$]. Heat-capacity calculations were made on a model-3600 Data Station interfaced to the DSC. Values of C_p for a synthetic sapphire sample determined in the same temperature range were within 1% of those in the literature.¹¹ The sample C_p values for $(\text{Me}_4)\text{N}^+(\text{HCTMCP})^-$ in Table I are of comparable accuracy.

The heat capacity of $(\text{Me}_4)\text{N}^+(\text{HCTMCP})^-$ between

TABLE I. Specific heat of $(\text{Me}_4)\text{N}^+(\text{HCTMCP})^-$.

T (K)	C_p ($\text{J mol}^{-1} \text{ K}^{-1}$)	T (K)	C_p ($\text{J mol}^{-1} \text{ K}^{-1}$)
255	396.1	325	480.6
265	408.2	335	493.9
275	419.6	345	511.6
285	431.5	355	530.9
295	442.6	365	521.6
305	455.6	375	499.3
315	466.9	385	507.9

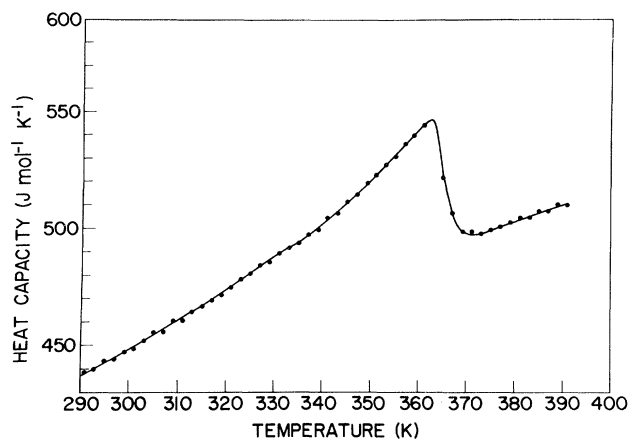


FIG. 3. Heat capacity of $(\text{Me}_4)\text{N}^+(\text{HCTMCP})^-$ between 290 and 391 K. Solid line smoothly connects the experimental values.

290 and 393 K is given in Fig. 3: The specific heat between 233 and 290 K extends the initial linear variation shown. A phase transition is clearly coincident with the magnetic transition and is found to be reversible, with an identical magnitude specific-heat anomaly upon heating or cooling. The specific heat first deviates from the extrapolated C_p behavior at lower temperatures on heating at about 334 K, reaching a maximum at 363.7 K. The finite slope above the transition temperature is a result of the 20-K min^{-1} scan rate. The enthalpy for a broadened first-order transition can be estimated by extrapolation from the high-temperature specific heat to lower temperatures and integrating the area under the anomaly, taking only the excess specific heat above the extrapolated baseline (see Fig. 3). The enthalpy change thus obtained is 1.35 kJ mol^{-1} corresponding to ΔS (the change in entropy) of $3.4 \text{ J mol}^{-1} \text{ K}^{-1}$. Treated as a second-order transition, the specific-heat discontinuity at 364 K of $56 \text{ J mol}^{-1} \text{ K}^{-1}$ considerably exceeds the $12.6 \text{ J mol}^{-1} \text{ K}^{-1}$ given by simple molecular-field theory for a second-order antiferromagnetic phase transition: This suggests that the transition involves not only the magnetic spins but is dominated by changes in the lattice vibrational energies.

THERMAL EXPANSION OF CRYSTAL LATTICE

The variation of lattice constants with temperature in $(\text{Me}_4)\text{N}^+(\text{HCTMCP})^-$ has been measured between 294.2

and 407.4 K. Experimentally, a single crystal was mounted within a microfurnace¹² set on an Enraf-Nonius CAD-4 diffractometer: 25 reflections with $20^\circ \leq 2\theta \leq 35^\circ$ were measured at each temperature with graphite-monochromated Mo $K\alpha$ radiation [$\lambda(K\alpha_{1,2}) = 0.70930$ and 0.71359 \AA]. Values of $2\theta(h,k,l) = \omega(h,k,l) - \omega(\bar{h}, \bar{k}, \bar{l})$ were measured in the bisecting mode with $\omega(\bar{h}, \bar{k}, \bar{l})$ at negative 2θ angles. Unit-cell dimensions were determined from the resulting set of 2θ values by the least-squares method.¹³

The crystal symmetry at room temperature is triclinic, with lattice dimensions at several temperatures sampled in Table II. The lengths of the a and b axes vary continuously with temperature and, as the phase transition is approached, reach a common value. The α - and β -lattice angles vary similarly. The temperature dependence of the two sets of dimensions is presented in Figs. 4 and 5. By contrast, the length of the c axis varies linearly with temperature between 294.2 and 407.4 K, as does the γ -lattice angle.

Each set of lattice dimensions may be fitted, by multiple linear-regression analysis, to a third-order polynomial of the form

$$a_i^T = a_i^{295 \text{ K}} [1 + A_i \Delta T + B_i (\Delta T)^2 + C_i (\Delta T)^3], \quad (1)$$

where $\Delta T = T - 295 \text{ K}$. The weights used in the regression analysis are the inverse of the sum of the experimental lattice constant and temperature variances. The resulting polynomial coefficients and standard lattice dimensions at 295 K are presented in Table III.

The intersection of the polynomial equation (1) for the a and b axes is at 365.4 K, and for the α and β angles it is at 365.1 K. The uncertainty in temperature at the crystal is estimated as 0.5 K, although the thermal stability is about one-half this value.¹² The mean phase-transition temperature of 365.3 K from the diffraction measurements is in good agreement both with the magnetic and specific-heat temperatures. It should be noted that the temperature dependence of the lattice dimensions very close to the transition temperature may differ significantly from that given by the coefficients in Table III.

The unit-cell volume varies linearly with temperature over the range 294.2–407.4 K, as in

$$V_T = V_{295 \text{ K}} [1 + 370(10) \Delta T \times 10^{-6} \text{ K}^{-1}], \quad (2)$$

TABLE II. $(\text{Me}_4)\text{N}^+(\text{HCTMCP})^-$ unit-cell dimensions between 294.2 and 397.6 K.

T (K)	a (Å)	b (Å)	c (Å)	α (deg)	β (deg)	γ (deg)	V (Å ³)
294.2	11.473(3)	12.002(3)	6.811(2)	104.55(2)	101.40(2)	67.85(2)	835.1(7)
312.2	11.526(3)	12.017(4)	6.832(4)	104.50(3)	101.71(4)	67.76(2)	841.7(10)
326.4	11.553(7)	11.990(5)	6.835(4)	104.43(4)	101.94(5)	67.66(4)	841.2(14)
340.4	11.616(5)	11.995(5)	6.865(4)	104.33(4)	102.28(4)	67.68(3)	849.8(13)
354.6	11.707(24)	11.926(24)	6.865(18)	103.83(19)	103.03(20)	67.71(17)	851.3(59)
369.0	11.834(8)	11.846(6)	6.899(3)	103.63(4)	103.58(5)	67.54(5)	857.1(13) ^a
388.2	11.883(8)	11.880(7)	6.913(6)	103.77(6)	103.77(6)	67.47(5)	863.5(20) ^a
407.4	11.890(6)	11.908(10)	6.929(3)	103.92(5)	103.90(4)	67.34(5)	866.5(15) ^a

^aVolume of transformed unit cell is double that given (see text).

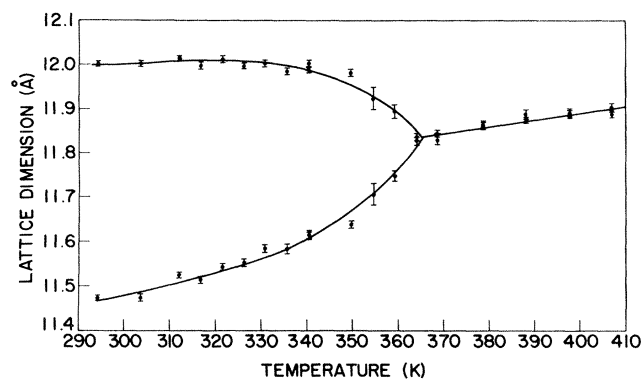


FIG. 4. Variation of the triclinic a - and b -axial lengths in $(\text{Me}_4)\text{N}^+(\text{HCTMCP})^-$ with temperature. Error bars are ± 1 e.s.d. Temperature uncertainty is estimated as ± 0.5 K. Solid line represents the fit to a cubic equation below and a linear equation above the phase transition, as given by Eq. (1), and may not adequately represent the behavior of these axial parameters very close to the phase-transition temperature.

assuming the crystal symmetry remains triclinic above the phase transition. The equalities $|\vec{a}| = |\vec{b}|$ and $\alpha = \beta$ in this temperature regime (see Table III or Figs. 4 and 5) and the results of Ref. 7 show the symmetry above the transition to be monoclinic. The resulting unit-cell translations are given by the matrix transformation $110/1\bar{1}0/001$. At 388.2 K, for example, the monoclinic unit cell has dimensions $a = 19.76(1)$, $b = 13.195(7)$, $c = 6.913(6)$ Å, and $\beta = 106.63(6)^\circ$ (with $\alpha = \gamma = 90^\circ$). This cell has a volume of 1727.1 \AA^3 , exactly double that of the corresponding triclinic cell. The monoclinic cell is C centered, with no additional allowed reciprocal-lattice points. The phase transition may hence be driven by a soft optical mode at a Brillouin-zone boundary that results in a doubling of the unit cell.¹⁴

STRUCTURAL PHASE TRANSITION

Single crystals grown from solution at room temperature are generally twin free, since each principal lattice

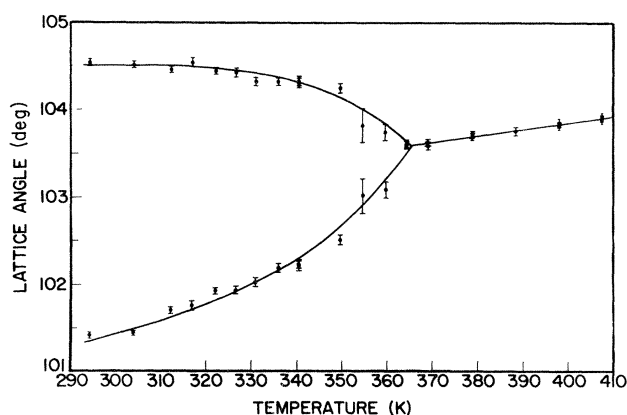


FIG. 5. Variation of the triclinic α - and β -lattice angles in $(\text{Me}_4)\text{N}^+(\text{HCTMCP})^-$ between 294 and 407 K. Also see caption to Fig. 4.

TABLE III. Thermal-expansion coefficients for $(\text{Me}_4)\text{N}^+(\text{HCTMCP})^-$; see Eq. (1) in text for the polynomial equation. Lattice constants at 295 K are $a = 11.470$ Å, $b = 12.003$ Å, $c = 6.808$ Å, $\alpha = 104.55^\circ$, $\beta = 101.38^\circ$, $\gamma = 67.84^\circ$, and $V = 834.5 \text{ \AA}^3$.

i	(a) Below phase transition		
	$A_i (10^{-6} \text{ K}^{-1})$	$B_i (10^{-6} \text{ K}^{-2})$	$C_i (10^{-9} \text{ K}^{-3})$
a	311(33)	-6.3(1.3)	118(13)
b	-60(34)	5.8(1.3)	-109(14)
c	172(3)		
α	-75(31)	2.9(1.2)	-52(12)
β	202(33)	-3.0(1.3)	65(13)
γ	-55(4)		
	(b) Above phase transition		
a, b	132(10)		
c^a	172(3)		
α, β	70(8)		
γ^a	-55(4)		

^aIdentical to coefficient value below phase transition.

direction is unique. Upon heating $(\text{Me}_4)\text{N}^+(\text{HCTMCP})^-$, the 0.53-\AA difference in length between \vec{a} and \vec{b} at 294 K gradually decreases to 0.44 \AA at 330 K and 0.28 \AA at 350 K, becoming zero at 365.4 K (see Fig. 4): The α and β angles vary similarly (see Fig. 5). Above the phase-transition temperature the \vec{a} and \vec{b} axial lengths remain identical, as do the α and β angles, presumably until the sharp onset of decomposition (corresponding to the loss in mass of three methyl groups) at 538 K which occurs without melting. The development of a choice in lattice orientation upon cooling through the phase transition, i.e., abc or bac , may be expected to produce twin domains at temperatures below but close to 365 K. At lower temperatures the strain developed between right- and left-handed twin domains is expected to become progressively larger. Microscopic hot-stage observation shows no color change at the phase transition: Some crystals exhibit minor fracture upon thermal cycling through the transition, and others are without apparent change. The average x-ray-diffraction line profile broadens upon cooling through the transition temperature.

It is of interest to note that the initial deviation from linearity in heat capacity at about 320 K coincides with the temperature at which the rate of change in $|\vec{a}| - |\vec{b}|$ starts increasing rapidly. The detailed changes in arrangement of the planar $(\text{HCTMCP})^-$ anions and $(\text{Me}_4)\text{N}^+$ cations at the phase transition will be discussed elsewhere.⁷

ACKNOWLEDGMENTS

It is a pleasure to thank P. K. Gallagher for the preliminary scanning calorimetry measurements in $(\text{Me}_4)\text{N}^+(\text{HCTMCP})^-$, R. Breslow for encouragement in synthesizing the material, and the National Science Foundation (Grant No. CHE-82-08569) for support of one of us (L.A.D.).

- ¹H. McConnell, Proc. Welch Found. Conf. Chem. Res. 11, 144 (1967). Also see quotation in Ref. 4.
- ²A. A. Ovchinnikov, Theor. Chim. Acta (Berlin) 47, 297 (1978).
- ³A. L. Buchachenko, Dokl. Akad. Nauk. SSSR 244, 1146 (1979).
- ⁴R. Breslow, Pure Appl. Chem. 54, 927 (1982).
- ⁵T. Fukunaga, J. Amer. Chem. Soc. 98, 610 (1976); U.S. Patent 3 963 769 (June 15, 1976).
- ⁶Inter-Society Color Council—(ISCC) National Bureau of Standards (NBS) Standard Color Supplement, NBS Circular No. 553 (1955) (unpublished).
- ⁷S. C. Abrahams, P. Marsh, and L. A. Deuring (to be published).
- ⁸J. C. Bonner and M. E. Fisher, Phys. Rev. 135, A640 (1964).
- ⁹R. E. Peierls, *Quantum Theory of Solids* (Oxford University Press, London, 1955).
- ¹⁰I. S. Jacobs, J. W. Bray, H. R. Hart, Jr., L. V. Interrante, J. S. Kasper, G. D. Watkins, D. R. Prober, and J. C. Bonner, Phys. Rev. B 14, 3036 (1976).
- ¹¹D. C. Ginnings and G. T. Furukawa, J. Amer. Chem. Soc. 75, 522 (1953).
- ¹²F. Lissalde, S. C. Abrahams, and J. L. Bernstein, J. Appl. Crystallogr. 11, 31 (1978).
- ¹³*Enraf-Nonius CAD-4 Manual* (Enraf-Nonius, Delft, The Netherlands, 1982).
- ¹⁴E. Pytte, Solid State Commun. 8, 2101 (1970).